Electronic Supplementary Material (ESI) for CrystEngComm.

Supplementary Information

Synchrotron x-ray diffraction characterization on inheritance of GaN homoepitaxial thin films grown on selective growth substrates

Yanfang Lou,[1,2] Chulho Song,[2] Yanna Chen,[2,3] Loku Singgappulige Rosantha Kumara,[2] Natalia Palina,[2] Okkyun Seo,[2,3] Satoshi Hiroi,[3] Kentaro Kajiwara,[4] Masato Hoshino,[4] Kentaro Uesugi,[4] Yoshihiro Irokawa,[1] Toshihide Nabatame,[1] Yasuo Koide,[1] and Osami Sakata[1,2,3,*]

[1]Center for GaN Characterization and Analysis,
Research Network and Facility Services Division (RNFS), National Institute for Materials Science (NIMS),
1-2-1 Sengen, Tsukuba, Ibaraki, 305-0047, Japan

[2]Synchrotron X-ray Station at SPring-8, RNFS, NIMS,
1-1-1 Kouto, Sayo-cho, Sayo-gun, Hyogo 679-5148, Japan

[3]Synchrotron X-ray Group, Research Center for Advanced Measurement and Characterization,
NIMS, 1-1-1 Kouto, Sayo-cho, Sayo-gun, Hyogo 679-5148, Japan

[4]Research & Utilization Division Japan Synchrotron Radiation Research Institute (JASRI),
1-1-1 Kouto, Sayo-cho, Sayo-gun, Hyogo 679-5198, Japan

* SAKATA.Osami@nims.go.jp; Corresponding author

Sample setup for monochromatic x ray topographic measurements

Figure S1 shows the schematic experimental setup for monochromatic x ray topographic measurements. The sample was rotated around the [1-100] axis to record the diffraction images for several set angels near the 11-24 Bragg angle with a fixed sample position, detector angle, and detector position. Synchrotron x rays having a wavelength of 1.284 Å were from a double-crystal Si (111) monochromator. The Bragg reflection geometry was used.

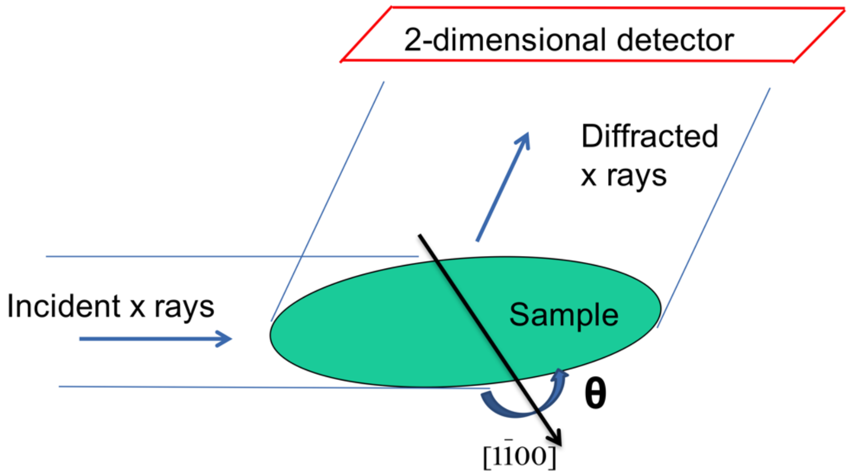

Figure S1. The Schematic diagram of monochromatic x-ray topography experiment setup.

Sample setup for white beam x ray topographic measurements

Figure S2 shows the schematic experimental setup for white beam diffraction measurements in transmission mode. The 11-20 diffraction was excited at the Bragg angle of 3˚ for an incident x rays with a wavelength of 0.1670 Å. The sample height and horizontal position was changed using a sample stage.

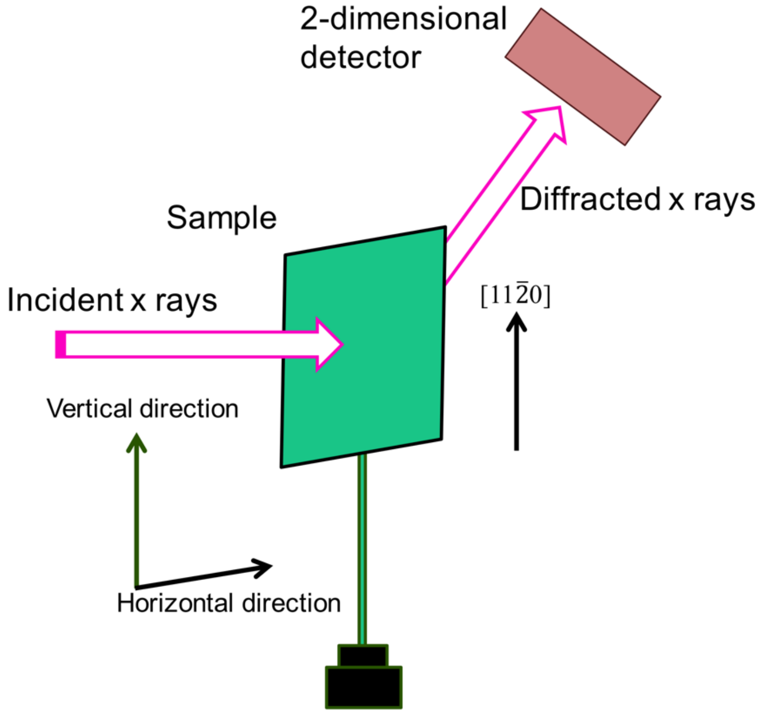

Figure S2. The Schematic diagram of white-beam x-ray topography experiment setup.

Angles and absolute reflectivities of sample S for rocking curves shown in Fig. 3d

Table S1 listed angular information and absolute reflectivity normalized by the incident x ray intensity for sample **S**. We refined the detector angle 2θand the incident x ray angleθfor the 0002 reflection. The incident x ray wavelength was 1.55 Å. The rocking curves of the points (Positions 1-6) have narrow widths and higher absolute reflectivities (around 80%), whereas those in the boundary region (Positions 7 and 8) had wider widths and lower absolute reflectivities (about 20%).

Table S1. The detailed information of rocking curves and absolute reflectivity for the selected areas from sample **S**.

Position	2θ(º)	θ(º)	FWHM(º)	Absolute reflectivity
1st	34.7875	17.3704	0.0056	0.855
2nd	34.7777	17.3721	0.0058	0.867
3rd	34.7716	17.3698	0.0059	0.835
4th	34.789	17.3693	0.0057	0.876
5th	34.7869	17.3709	0.0063	0.803
6th	34.7866	17.3722	0.0061	0.847
7th	34.7859	17.3723	0.0158	0.282
8th	34.7853	17.3661	0.0136	0.305

Angles and absolute reflectivities of sample N for rocking curves shown in Fig. 4c

Table S2 listed angular information and absolute reflectivity normalized by the incident x ray intensity for sample **N**. We refined the detector angle 2θand the incident x ray angleθfor the 0002 reflection. The incident x ray wavelength was 1.55 Å. All the rocking curves are broader and the absolute reflectivities are lower (around 40%).

Table S2. The detailed information of rocking curves and absolute reflectivity for the selected areas from sample **N**.

Position	2θ(º)	θ(º)	FWHM(º)	Absolute reflectivity
1st	34.7885	18.3379	0.0168	0.267
2nd	34.7878	18.3612	0.0222	0.284
3rd	34.7869	18.3258	0.0128	0.416
4th	34.7871	18.3424	0.0065	0.700
5th	34.7881	18.3426	0.0105	0.414
6th	34.7882	18.3331	0.0127	0.385

Diffraction intensity images as a function of sample height from samples S and N

Figure S3 shows intensity profiles for sample different vertical positions as a function of sample horizontal position. The images from samples **S** and **N** exhibit similar regularities, indicating the main features of sample **S** were inherited by **N**.

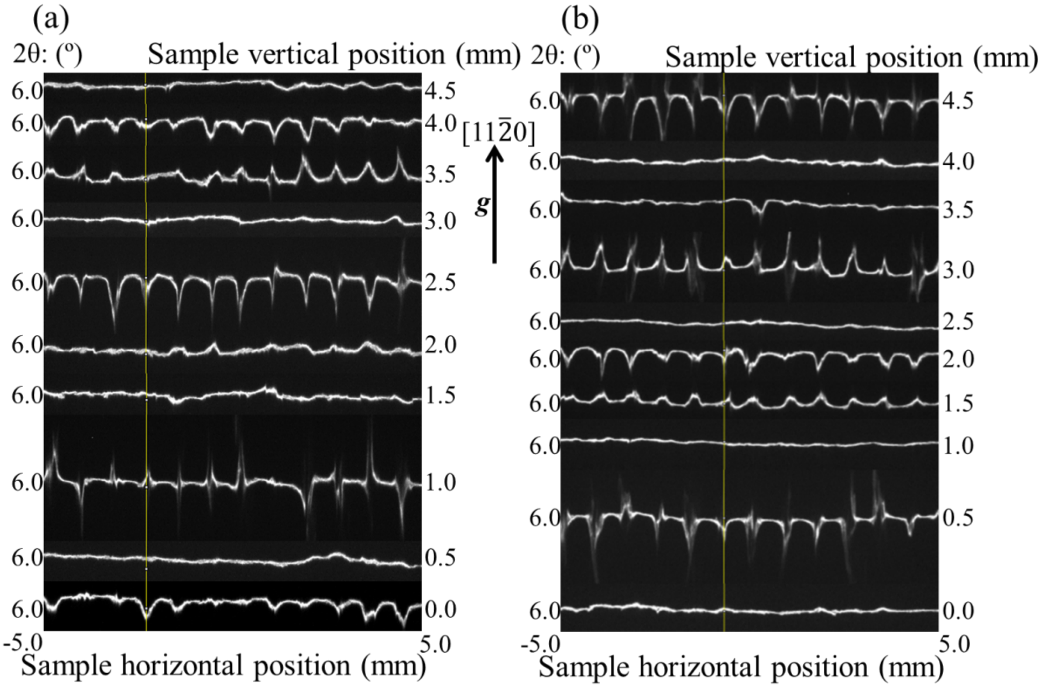

Figure S3. White-beam x ray topographic images with vertical direction changed in case of a beam size of 0.01 mm (height) × 10 mm (lateral) from (a) sample **S** and (b) sample **N**.

Diffraction intensity images as a function of sample height from samples P1 and P2

Figure S4 shows intensity profiles for sample different vertical positions as a function of sample horizontal position. The images from the group for sample **P** looks to have less regularity and an inhomogeneous structure.

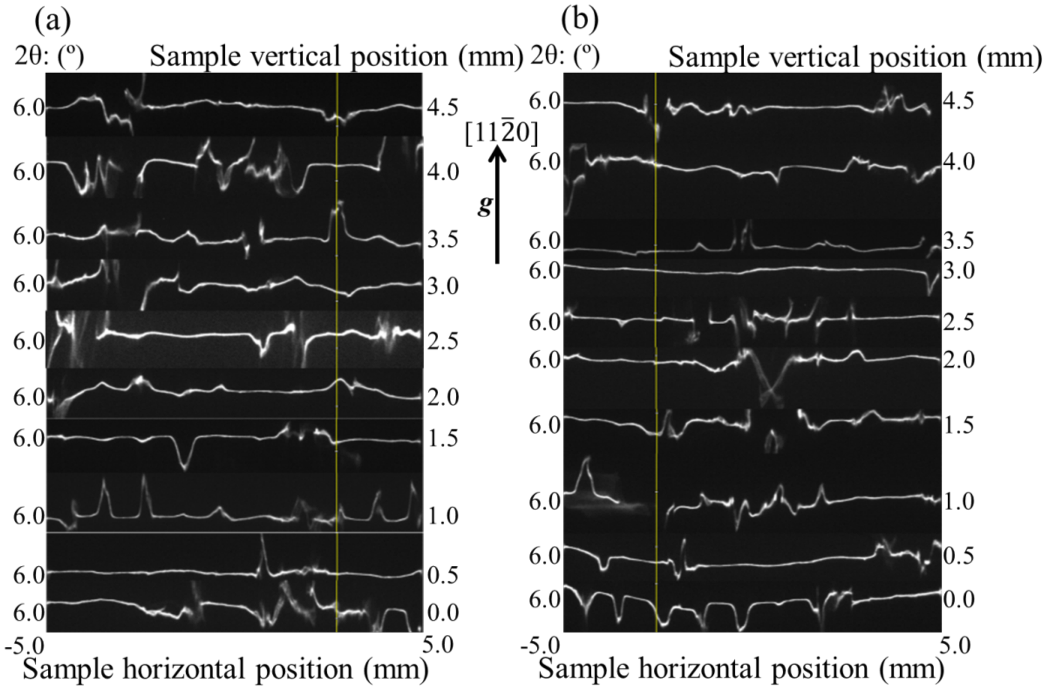

Figure S4. White-beam x-ray topographic images with vertical direction changed in case of a beam size of 0.01 mm (height) × 10 mm (lateral) from (a) sample **P**1, (b) sample **P**2. Samples **P**1 and **P**2 were cut from adjacent areas on the same wafer.